A MINIMUM-MASS EXTRASOLAR NEBULA

MARC J. KUCHNER[1]
Princeton University Observatory, Peyton Hall, Princeton, NJ 08544; mkuchner@astro.princeton.edu

ABSTRACT

By analogy with the minimum-mass solar nebula, we construct a surface-density profile using the orbits of the 26 precise-Doppler planets found in multiple-planet systems: $\Sigma = 2200 \, (a/1 \text{ AU})^{-\beta}$ g cm^{-2}, where a is the circumstellar radius and $\beta = 2.0 \pm 0.5$. The minimum-mass solar nebula ($\beta = 1.5$) is consistent with this model, but the uniform-α accretion disk model ($\beta \approx 1$) is not. In a nebula with $\beta > 2$, the center of the disk is the likely cradle of planet formation.

Subject headings: planetary systems: protoplanetary disks — solar system: formation

1. INTRODUCTION

Our understanding of the mass profile of the disk from which the planets of the solar system formed begins with the minimum-mass solar nebula (MMSN). Imagine adding just enough light elements to each planet so that all the planets reach solar composition, then smearing the augmented planets into contiguous nested rings (Edgeworth 1949; Kuiper 1956; Safronov 1967; Alfvén & Arrhenius 1970; Kusaka et al. 1970; Lecar & Franklin 1973). Fitting a power law to the resulting surface-density distribution leads to the well-known MMSN prescription, $\Sigma = \Sigma_0 (a/1 \text{ AU})^{-3/2}$, where Σ is the surface density and a is the circumstellar radius (Weidenschilling 1977; Hayashi 1981).

The estimates of Weidenschilling (1977) for the masses of the planets augmented to solar composition suggest that $\Sigma_0 \approx 4200$ g cm^{-2}. Using the same table of solar abundances (Cameron 1973) but making some additional assumptions about the importance of the snow line, Hayashi (1981) derived $\Sigma_0 = 1700$ g cm^{-2}. Since the snow line's location and role in giant planet formation are uncertain (Sasselov & Lecar 2000), we prefer the above formula based on Weidenschilling (1977) for the purposes of this paper.

Elaborate calculations of planet formation (e.g., Trilling et al. 1998; Ida & Lin 2004) regularly invoke the MMSN or a $\Sigma \approx a^{-1}$ surface density distribution based on uniform-α accretion disk models (Shakura & Sunyaev 1973). Such calculations can depend strongly on the assumed surface-density distribution. For example, the isolation mass produced by runaway planetesimal growth goes as $\Sigma^{3/2}$ (Lissauer 1987). The locations of secular resonances in the nebula are especially sensitive to the surface-density distribution (Lecar & Franklin 1997; Nagasawa & Ida 2000).

Now, newly discovered extrasolar planets outnumber the solar system planets. This paper attempts to update our picture of the minimum-mass nebula taking the extrasolar planets into account; we derive a surface-density profile analogous to the MMSN using the orbits of the 26 extrasolar planets found in multiple-planet systems. Perhaps this new construction—a minimum-mass extrasolar nebula (MMEN)—can serve future studies of planet formation.

2. DATA

The extrasolar planets discovered so far by precise-Doppler methods contain nine two-planet systems and two three-planet systems. We obtained the orbital data for these planets from the California and Carnegie Planet Search Web site;[2] see the review by Marcy & Butler (2000) for background on radial velocity planet searches. Table 1 summarizes the relevant data on these systems, including measured stellar metallicities from Santos et al. (2004). Of the 11 listed extrasolar planet host stars, 8 are G type.

Besides multiple systems inferred purely from radial velocity observations, the table also includes ϵ Eri. This system contains one planet inferred from radial velocity measurements to have a semimajor axis of 3.3 AU and a second planet inferred from the structure of a circumstellar debris disk imaged in the submillimeter (Greaves et al. 1998; Quillen & Thorndike 2002; Kuchner & Holman 2003). Quillen & Thorndike (2002), estimate that this second planet has a semimajor axis of 40 AU and a mass of 10^{-4} times the mass of ϵ Eri (0.8 $M_\odot$). Since the existence of these planets is still debated, we perform our analysis both with and without them in the sample.

Radial velocity surveys are generally biased against detecting low-mass planets at large periods. Precise-Doppler surveys can currently detect radial velocity variations with amplitude $\gtrsim 3$ m s^{-1}. In terms of the planet's orbital period, P, and the ratio of the mass of the planet to the mass of the star, μ, this detection limit corresponds to

$$\mu \sin i \geq 10^{-4} \left(\frac{P}{1 \text{ yr}} \right)^{1/3} \left(\frac{M}{M_\odot} \right)^{-1/3}, \qquad (1)$$

where i is the inclination of the normal to the planet's orbital plane to the line of sight.

Figure 1 shows the orbital period and $\mu \sin i$ of each planet. Open circles indicate planets in two-planet systems. Filled circles indicate planets in three-planet systems. The triangles indicate the ϵ Eri planets. The solid line shows the 3 m s^{-1} detection limit, calculated for a 1 $M_\odot$ star. For the purpose of Figure 1, we assume $\sin i = 0.5$ for ϵ Eri based on the inclination of the disk.

This figure suggests that the detection bias in this data set is likely to be small; all of the precise-Doppler planets in our data set could have been detected out to the period limit (roughly 10 yr), except for 55 Cnc c, which could have been detected only out to a period of 6 yr. However, other

---

[1] Hubble Fellow.

[2] Available at http://www.exoplanets.org.

TABLE 1
MULTIPLE-PLANET SYSTEMS

Star	Spectral Type	[Fe/H]	Semimajor Axes (AU)	Σ_0 (g cm^{-2})	β
Sun	G2 V	0.0	5.20, 9.54, 19.19, 30.07	4225	1.78
55 Cnc......................	G8 V	0.33 ± 0.07	0.115, 0.24, 5.9	739	2.42
υ And	F8 V	0.13 ± 0.08	0.059, 0.829, 2.53	2670	1.50
GJ876	M4	0.0[a]	0.13, 0.21	8634	2.00
HD 38529	G4 IV	0.40 ± 0.06	0.129, 3.71	705	1.58
HD 82943	G0	0.30	0.728, 1.16	8907	2.00
HD 169830	F8 V	0.21 ± 0.05	0.81, 3.60	2815	2.00
HD 12661	G6 V	0.36 ± 0.05	0.82, 2.6	3013	2.00
HD 168443	G5 IV	0.06 ± 0.05	0.295, 2.87	3374	1.65
HD 74156	G0	0.16 ± 0.05	0.294, 3.40	1012	1.63
47 UMa...................	G0 V	0.06 ± 0.03	2.89, 3.73	7026	2.00
HD 37124	G4 V	-0.38 ± 0.04	0.54, 2.5	1949	2.00
ϵ Eri........................	K7 V	-0.13 ± 0.04	3.3, 40.0	715	2.00

[a] From http://www.exoplanets.org.

biases might lurk in the process of reporting and publishing the exoplanet data, and naturally, detecting planets via disk perturbations suffers from a special set of biases. Our analysis begs repeating when more data become available.

3. ANALYSIS

Constructing a MMEN from these data requires associating a surface density with each extrasolar planet. To derive these surface densities, we first must estimate an augmented mass for each planet—the mass each planet would have if it accreted just enough additional gas with the right chemistry so that it attained solar composition. We can convert the augmented mass to a surface density based on the spacings of the planets in multiple-planet systems.

Jupiter has a mass of 318 $M_\bullet$ and roughly 2–4 times solar abundances of C, N, and S (Gautier et al. 2001), suggesting that its augmented mass should be roughly 1000 $M_\bullet$. Estimates for the augmented masses of Saturn, Uranus, and Neptune are all

FIG. 1.—Orbital period and $\mu \sin i$ for the extrasolar planets in multiple-planet systems; μ is the ratio of the mass of the planet to the mass of the star. Open circles indicate planets in two-planet systems, and filled circles indicate planets in three-planet systems. Two triangles indicate the ϵ Eri planets. The solid line shows the 3 m s^{-1} radial velocity detection limit for a 1 $M_\odot$ star, comfortably below $\mu \sin i$ for most of our sample.

consistent with this value, even though their actual masses span a factor of $\sim$20 (Weidenschilling 1977). This trend supports a planet formation scenario in which the observed range of planet masses arises mainly from variations in volatile depletion.

We chose 1000 $M_\bullet$ for the augmented masses of most of the extrasolar planets. If we try to construct the minimum-mass solar nebula from the orbits of Jupiter, Saturn, Uranus, and Neptune under this approximation, we get $\Sigma = 4230 (a/1 \text{ AU})^{-1.8}$ g cm^{-2}, in rough agreement with the MMSN of Weidenschilling (1977). A few planet candidates have measured minimum masses greater than 1000 $M_\bullet$: HD 168443b ($m \sin i = 7.73 M_J$), HD 168443c ($m \sin i = 17.2 M_J$), HD 74156c ($m \sin i = 8.21 M_J$), υ And d ($m \sin i = 3.75 M_J$), and 55 Cnc d ($m \sin i = 4.05 M_J$). We used the measured minimum masses, $m \sin i$, as the augmented masses for these planets. Using $m \sin i$ for all the augmented masses would substantially increase the dispersion in the surface densities.

To derive surface densities, we divided each planet's augmented mass by the area of an appropriate annulus. Here we harnessed the multiple-planet systems; we used the separation of the planets in log semimajor axis space as the full width of each annulus. In other words, we chose the boundaries of the annuli to be the geometric means of the adjacent semimajor axes. Weidenschilling (1977) found that using an arithmetic mean or a geometric mean generated indistinguishable results for the solar system. However, the larger separations of the extrasolar planets seem to call for the use of the geometric mean, given the usual picture of feeding zones for planetary accretion that span widths measured in units of the local Hill radius (e.g., Kokubo & Ida 1998). The extrasolar planets exhibit a much larger range of orbital eccentricities than the solar planets (Marcy & Butler 2000); we do not attempt to take this factor into account.

Figure 2 shows the surface densities we associate with each planet. Open circles indicate the surface densities associated with the planets in two-planet systems. Filled circles indicate the surface densities associated with the planets in three-planet systems. Also plotted are surface densities associated with the ϵ Eri planets, marked by triangles.

Table 1 reveals some of the subtleties of this procedure. It lists the parameters Σ_0 and β for minimum-mass nebulae fitted separately to each system. The table shows that $\beta = 2$ for any two-planet system in which both planets have the same mass;
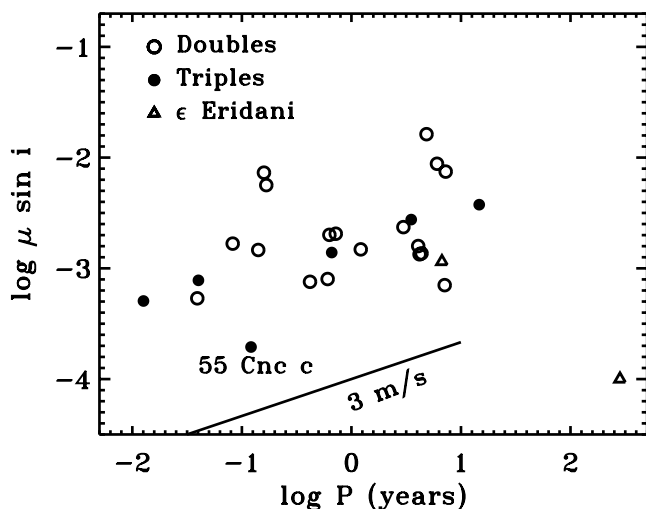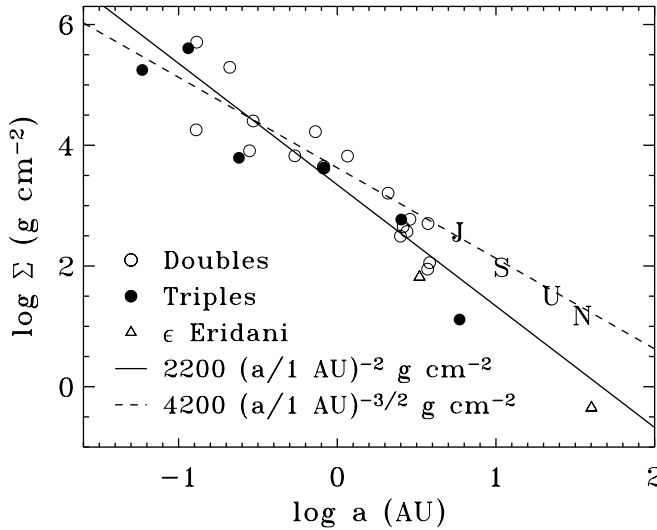
FIG. 2.—Extrasolar planet surface densities. Filled circles are planets in three-planet systems, and open circles are two-planet systems. Two triangles indicate the ϵ Eri planets. The best-fit power law is a^{-2} (*solid line*), although $a^{-3/2}$ (*dashed line*) is also marginally consistent with the data.

this limitation of the algorithm prevents us from taking the separately fitted nebulae too seriously or subdividing the data set in too much detail.

The table also shows that the metallicities of the host stars range over 0.67 dex. At first, one might wonder how this spread in metallicity should affect the augmented masses. However, it turns out that for power-law models fitted without any attempt to take stellar metallicity into account, Σ_0 shows no correlation with stellar metallicity, only scatter. This lack of a discernible trend suggests that metallicity corrections are beneath the fidelity of our method.

Table 2 shows Σ_0 and β for power laws fitted to the data taken as a whole and to subsets of the data. The power law best fit to the whole data set has the form $\Sigma = 2200 \, (a/1 \text{ AU})^{-2.0} \text{ g cm}^{-2}$. This form for the MMEN has a total mass of $8M_J$ in the region 0.3–30 AU, compared to $31M_J$ for the MMSN. This difference may result from the current inability of radial velocity techniques to measure orbital periods longer than $\sim$10 yr; we may have only found one-third of the mass we will eventually find.

Figure 2 compares the above form for the MMEN (*solid line*) with the standard MMSN, $\Sigma = 4200 \, (a/1 \text{ AU})^{-3/2} \text{ g cm}^{-2}$ (*dashed line*). Assuming that the logarithms of the surface densities have uncertainties of ± 0.3, the uncertainty in the exponent of the power-law fit to the entire data set is $\beta = 2 \pm 0.5$. Given these assumptions, the standard MMSN is consistent with the exoplanet data.

TABLE 2
BEST-FIT SURFACE-DENSITY PROFILES

Data Set	Σ_0 (g cm^{-2})	β
Two-planet systems only	2990	1.87
Three-planet systems only	739	2.42
G-star exoplanets only	2150	1.79
All exoplanets but ϵ Eri	2500	1.87
All exoplanets	2220	2.01
Solar system giants only	4230	1.78
Exoplanets + solar system giants	2490	1.87

4. DISCUSSION

4.1. *Other Nebular Models*

By combining the data from several exoplanet systems, we have implicitly assumed that protoplanetary disks have a common surface-density distribution. Such a common profile might stem from a steady state model of the protoplanetary accretion disk, like the uniform-α accretion disk model (Shakura & Sunyaev 1973).

However, the uniform-α accretion disk model ($\beta \approx 1$) is not consistent with the MMEN power law, and perhaps we should not expect it to be. The primary justification for this model is that a uniform α is the simplest assumption one can make about anomalous disk viscosity. However, the reason for angular momentum transport in disks is highly debated; models of disk turbulence driven by magnetorotational instability (e.g., Fleming & Stone 2002) suggest that the angular momentum transport is highly nonuniform, and may not even be characterized by a viscosity.

Another steady state disk model is a massive circumstellar disk bordering on gravitational instability. Spiral density waves may form in these disks that tend to redistribute angular momentum to maintain Toomre's Q at $\sim$1 throughout the disk (Laughlin & Bodenheimer 1994). Alternatively, planets could conceivably form via direct gravitational collapse of such disks (e.g., Boss 2001), depending on the thermodynamic assumptions (Pickett et al. 2000). For a disk with uniform Q, the surface density profile is determined by the square root of the local disk temperature, so a variety of disk thermal models would yield similar surface-density distributions. These disks are at least an order of magnitude more massive than the minimum-mass nebulae we are considering. For example, a $Q = 1$ disk where the midplane temperature is $T = 150 \, (a/1 \text{ AU})^{-3/7}$ K (Chiang & Goldreich 1997) has surface density $\Sigma = 88000 \, (a/1 \text{ AU})^{-1.93} \text{ g cm}^{-2}$.

Of course, the real solar nebula may seldom have been near a steady state; T Tauri stars are highly variable, and at any given stellar age, one can find stars both with and without accretion disks in the same cluster (e.g., Haisch et al. 2001). One-dimensional models of protoplanetary disk accretion more sophisticated than the uniform-α model (Gammie 1996; Matsuyama et al. 2003) generate time-variable surface-density profiles. Ironically, these models often use the MMSN as a starting point. In general, a non–steady state picture of the protoplanetary disk stretches our interpretation of the MMSN and MMEN; all of the inferred minimum mass may not have been present in the disk at the same time.

4.2. *A Steeper Surface-Density Distribution?*

Although taken as a whole, the extrasolar planet data agree with the MMSN, Figure 2 and Table 2 show that some extrasolar planetary systems themselves do not. The β exponents for the three-exoplanet systems and for the solar system differ substantially; the minimum-mass nebula constructed from the three-exoplanet systems has more mass concentrated in the center, like the uniform-Q model mentioned above. These three-exoplanet systems are the ones for which our algorithm works the best.

Conventional wisdom holds that giant planets form at 2–5 AU from the star, perhaps at the snow line, and that the close-in extrasolar planets migrated inward from where they formed (Lin et al. 1996). According to this picture, one might expect the MMEN to be more centrally peaked than the MMSN. Perhaps the reason for the steep power law among

the three-exoplanet systems is that these planets are more widely separated in semimajor axis than planets in the solar system; with our prescription, increasing planet separations steepens the power law. The planet-disk interactions that cause the planets to migrate to small a could create the wider separations; massive planets can clear out the region between them in a protoplanetary disk via slowly damped spiral density waves (Bryden et al. 2000), preventing more planets for growing in these regions.

5. INSIDE-OUT PLANET FORMATION

However, looking at things another way, the steeper nebular surface density distributions consistent with the MMEN could have dramatic implications for where planets are formed. Let us briefly indulge this alternative viewpoint.

An annulus of the protoplanetary disk with width Δr has mass $m = 2\pi\Sigma r\Delta r$. If this annulus is a feeding zone with $\Delta r \propto r$ and if $\Sigma \propto r^{-\beta}$, then $m \propto r^{2-\beta}$. For the minimum-mass solar nebula ($\beta = 1.5$) and uniform-α disk model ($\beta \approx 1$), m increases with radius, suggesting that more mass is available for planet formation at larger distances from the star. This tale—an exercise in circular reasoning—has been a standard argument for why giant planets ought not to form predominantly at the center of the disk.

However, for $\beta > 2$, m decreases with radius, suggesting that the center of the disk is the most natural site for planet formation. Perhaps giant planets predominantly form in the center of their disks and migrate outward.

Indeed, suitable outward migration mechanisms for giant planets exist: type III migration (Masset & Papaloizou 2003) and planet-planet scattering (Thommes et al. 1999; Adams & Laughlin 2003). Type III migration begins when the planet grows larger than a threshold mass sufficient to begin opening a gap in the disk (Artymowicz 2004). Some planet-planet interactions may also be required to produce the observed range of extrasolar planet orbital eccentricities.

Outward type III migration will halt at the outer boundary of the disk. Matsuyama et al. (2003) have suggested that the disk may develop an edge or a gap at ~5 AU when the photoevaporation timescale matches the viscous spreading timescale. The exact nature and location of this edge remain uncertain. However, the disk probably photoevaporates first outside ~5 AU, providing a natural stopping place for outward planet migration.

This inside-out planet-formation scenario has several attractive features. While no direct observational evidence has yet been found for a special structure at the snow line in protoplanetary disks, abundant new evidence from near-infrared spectroscopy (Hartmann et al. 1993; Muzerolle et al. 2003) and interferometry (Millan-Gabet et al. 2001; Colavita et al. 2003) implies that T Tauri disks have dramatic opacity jumps at ~0.1 AU. Models of layered accretion disks (Gammie 1996; Armitage et al. 2001) suggest that even while most of the disk has $Q \gg 1$, the center of the disk could become gravitationally unstable, fostering planet formation by disk instability. Moreover, formation of the planets in the center of the disk could potentially solve two problems in the core accretion picture:

1. *Type I migration of giant planet cores.*—Conventional simulations of the semimajor axis distribution of the extrasolar planets (Trilling et al. 2002; Armitage et al. 2002; Ida & Lin 2004) neglect type I migration (Ward 1997) on the grounds that no planets could form at the snow line if this mechanism operated. Although present calculations of the migration of

small bodies do not accurately include torques added in the coorbital region (Bate et al. 2003), these torques are likely to dominate the net Lindblad torque, not compensate for it, exacerbating the problem. However, several mechanisms have been suggested that could stop migration of cores in the center of the disk (Lin et al. 1996; Kuchner & Lecar 2002; Terquem 2003; Laughlin et al. 2004; Nelson & Papaloizou 2004).

2. *The missing short-period pileup.*—Tabachnik & Tremaine (2002) and Tremaine & Zakamska (2004) pointed out that the distribution of planet orbital periods shorter than ~200 days is consistent with a power law, and that scenarios in which planets migrate inward and stop migrating at a special small orbital period should produce a much larger pileup of planets at short periods than observed. Gu et al. (2003) invoked tidal-driven Roche lobe overflow to remove this exaggerated pileup of planets in 3 day orbits expected from Monte Carlo migration models. However, most of the stopping mechanisms cited above are not specific to precisely 3 day periods, and since tidal forces decay as a^{-6}, tide-induced Roche lobe overflow can probably not help prevent pileups at say, a 6 day period. If planets mostly migrated outward when they grew beyond a threshold mass as type III accretion models suggest, this missing pileup problem would not arise.

Two effects make the very center of the disk (0.05–0.1 AU) problematic for core accretion: heating of the planet by tidal interaction with the star (Gu et al. 2003) and the large critical core radius for gas accretion at high nebular temperatures (Bodenheimer et al. 2000). However, the region at ~0.2 AU could be fertile ground for planet formation by either core accretion or disk instability. The disk temperature there is potentially low enough that the critical core radius shrinks to where it is consistent with the inferred core mass of Jupiter and Saturn (Papaloizou & Terquem 1999; Ikoma et al. 2001), particularly if this region is shadowed by a puffed-up inner wall of the disk (Natta et al. 2001; Dullemond et al. 2001). Conceivably, the observed extrasolar planets all could have formed at 0.1–0.2 AU and migrated to their current orbits. The solar system giants might also have formed via this process, although this possibility raises the question of the origin of the abundant low-temperature condensates in the envelopes of these planets (e.g., Gautier et al. 2001), a question still inadequately answered by any planet-formation model.

6. CONCLUSIONS

By analogy with the minimum-mass solar nebula (MMSN), we constructed the surface-density distribution for a minimum-mass extrasolar nebula (MMEN) based on the orbits of the extrasolar planets in two- and three-planet systems: $\Sigma \approx 2200$ $(a/1\ \mathrm{AU})^{-2}$ g cm^{-2}. The standard MMSN is consistent with the exoplanet data taken as a whole, although the uniform-α accretion disk (Shakura & Sunyaev 1973) is not.

In general, although the MMSN is consistent with the MMEN, our analysis illustrates that the logic that led to the MMSN supports a wide range of disk surface-density profiles, none of which can serve as a complete picture. The MMSN was based on Laplace's concept of the solar nebula as a smooth disk that broke up into rings that condensed into planets. In contrast, true protoplanetary disks are likely actively accreting and time variable.

Our analysis led us to consider the ramifications of alternative surface-density distributions. We pointed out that in the centrally concentrated nebular model suggested by the three-exoplanet systems, the center of the disk is the preferred site

for planet formation. The extrasolar giant planets—and possibly the giant planets of the solar system—could have formed at 0.1–0.2 AU and migrated to their present orbits via type III migration and planet-planet scattering.

Our simple model is not intended to replace the MMSN, but to illuminate its shortcomings and to expose our solar-centrism. We must not remain chained to $\beta = 1.5$; minimum mass can sometimes mean maximum prejudice.

REFERENCES

Adams, F. C., & Laughlin, G. 2003, Icarus, 163, 290
Alfvén, H., & Arrhenius, G. 1970, Ap&SS, 8, 338
Armitage, P. J., Livio, M., Lubow, S. H., & Pringle, J. E. 2002, MNRAS, 334, 248
Armitage, P. J., Livio, M., & Pringle, J. E. 2001, MNRAS, 324, 705
Artymowicz, P. 2004, Paper presented at KITP Conference: Planet Formation: Terrestrial and Extra Solar (Santa Barbara: Kavli Institute for Theoretical Physics), http://online.itp.ucsb.edu/online/planetf_c04/artymowicz/
Bate, M. R., Lubow, S. H., Ogilvie, G. I., & Miller, K. A. 2003, MNRAS, 341, 213
Bodenheimer, P., Hubickyj, O., & Lissauer, J. 2000, Icarus, 143, 2
Boss, A. 2001, ApJ, 563, 367
Bryden, G., Rozyczka, M., Lin, D. N. C., & Bodenheimer, P. 2000, ApJ, 540, 1091
Cameron, A. G. W. 1973, Space Sci. Rev., 15, 121
Chiang, E., & Goldreich, P. 1997, ApJ, 490, 368
Colavita, M., et al. 2003, ApJ, 592, L83
Dullemond, C. P., Dominik, C., & Natta, A. 2001, ApJ, 560, 957
Edgeworth, K. E. 1949, MNRAS, 109, 600
Fleming, T., & Stone, J. M. 2002, ApJ, 585, 908
Gammie, C. F. 1996, ApJ, 462, 725
Gautier, D., Hersant, F., Mousis, O., & Lunine, J. I. 2001, ApJ, 550, L227
Greaves, J. S., et al. 1998, ApJ, 506, L133
Gu, P.-G., Lin, D. N. C., & Bodenheimer, P. H. 2003, ApJ, 588, 509
Haisch, K. E., Lada, E. A., & Lada, C. J. 2001, ApJ, 553, L153
Hartmann, L., Kenyon, S. J., & Calvet, N. 1993, ApJ, 407, 219
Hayashi, C. 1981, Prog. Theor. Phys. Suppl., 70, 35
Ida, S., & Lin, D. N. C. 2004, ApJ, 604, 388
Ikoma, M., Emori, H., & Nakazawa, K. 2001, ApJ, 553, 999
Kokubo, E., & Ida, S. 1998, Icarus, 131, 171
Kuchner, M. J., & Holman, M. J. 2003, ApJ, 588, 1110
Kuchner, M. J., & Lecar, M. 2002, ApJ, 574, L87
Kuiper, G. P. 1956, JRASC, 50, 158
Kusaka, T., Nakano, T., & Hayashi, C. 1970, Prog. Theor. Phys., 44, 1580
Laughlin, G., & Bodenheimer, P. 1994, ApJ, 436, 335
Laughlin, G., Steinacker, A., & Adams, F. 2004, ApJ, 608, 489
Lecar, M., & Franklin, F. 1973, Icarus, 20, 422
———. 1997, Icarus, 129, 134
Lin, D. N. C., Bodenheimer, P., & Richardson, D. C. 1996, Nature, 380, 606
Lissauer, J. J. 1987, Icarus, 69, 249
Marcy, G. W., & Butler, R. P. 2000, PASP, 12, 137
Masset, F. S., & Papaloizou, J. C. B. 2003, ApJ, 588, 494
Matsuyama, I., Johnstone, D., & Murray, N. 2003, ApJ, 585, L143
Millan-Gabet, R., Schloerb, F. P., & Traub, W. A. 2001, ApJ, 546, 354
Muzerolle, J., Calvet, N., Hartmann, L., D'Alessio, P. 2003, ApJ, 597, L149
Nagasawa, M., & Ida, S. 2000, AJ, 120, 3311
Natta, A., Prusti, T., Neri, R., Wooden, D., Grini, V. P., & Mannings, V. 2001, A&A, 371, 186
Nelson, R. P., & Papaloizou, J. C. B. 2004, MNRAS, 350, 849
Papaloizou, J. C., & Terquem, C. 1999, ApJ, 521, 823
Pickett, B. K., Cassen, P., Durisen, R. H., & Link, R. 2000, ApJ, 529, 1034
Quillen, A. C., & Thorndike, S. 2002, ApJ, 578, L149
Safronov, V. S. 1967, Soviet Astron., 10, 650
Santos, N. C., Israelian, G., & Mayor, M. 2004, A&A, 415, 1153
Sasselov, D. D., & Lecar, M. 2000, ApJ, 528, 995
Shakura, N. I., & Sunyaev, R. A. 1973, A&A, 24, 337
Tabachnik, S., & Tremaine, S. 2002, MNRAS, 335, 151
Terquem, C. E. J. M. L. J. 2003, MNRAS, 341, 1157
Thommes, E. W., Duncan, M. J., & Levison, H. F. 1999, Nature, 402, 635
Tremaine, S., & Zakamska, N. L. 2004, in AIP Conf. Proc. 713, The Search for Other Worlds (New York: AIP), 243
Trilling, D. E., Lunine, J. I., & Benz, W. 2002, A&A, 394, 241
Trilling, D. E., et al. 1998, ApJ, 500, 428
Ward, W. R. 1997, ApJ, 482, L211
Weidenschilling, S. J. 1977, Ap&SS, 51, 153